ISSN 0540-469X

MITSUBISHI TECHNICAL BULLETIN No.201

Development of New Corrosion Resistant Stainless Steel for Sulphuric Acid Plant

September 1996

MITSUBISHI HEAVY INDUSTRIES, LTD.

Development of New Corrosion Resistant Stainless Steel for Sulphuric Acid Plant

Ryuichiro Ebara*1 Yoshikazu Yamada*1
Makoto Nakamura*2 Hajime Nagano*3
Tatsushi Hirai*4

We have successfully developed new corrosion resistant stainless steel with 6.5% silicon and 0.01% palladium for use with high-temperature sulphuric acid with more than 98 mass% at high temperatures up to 473 K in order to get a lighter and smaller structure and realize a heat recovery system. In this study, we have clarified the effects of the palladium and silicon content on the corrosion resistance of the newly developed steel. This steel can be easily produced by mill rolling to give an adjustable soaking treatment even when containing more than 6.5% silicon. The ductility of welded joints can be maintained by introducing an adjustable ferrite into the microstructure and the welded joint so that sufficient ductility can be provided by TIG welding.

1. Introduction

In recent years an effective heat recovery system is being realized and machines lighter in weight and smaller in size are being adopted in large-size sulphuric acid plants. Hence, stainless steel is taking the place of conventional material, carbon steel with acid-resistant brick lining for the process line and machines in such plants[1]. In order to materialize heat recovery system, the absorption tower, pump, tank, etc. will have to be put to work in sulphuric acid with temperature of 373 to 473 K and with concentration of 98 to 100% higher than the conventional levels. Therefore, the materials for machines to be used in such plants are specified to have substantial workability and weldability as well as excellent corrosion resistance.

The high-Si cast iron with Si content above 14% is well known to show excellent corrosion resistance against sulphuric acid plant environment. It has been reported lately, however, that the high-Cr ferritic stainless steel and the austenitic stainless steel with 5% silicon have comparatively excellent corrosion resistance[1]. However, high-Si cast iron and high-Cr ferritic stainless steel have inadequate workability and weldability, while the high-Si austenitic stainless steel is poor in corrosion resistance. Therefore, Mitsubishi Heavy Industries, Ltd. (MHI) launched development of a new corrosion resistant steel to meet the aforementioned requirements, and with the cooperation of NKK CORPORATION, has successfully developed the new corrosion resistant high-Si stainless steel containing palladium. This paper describes the newly developed stainless steel.

2. Chemical composition of new corrosion resistant stainless steel

The chemical composition of the newly developed steel is given in **Table 1**. The steel, with 17 Cr-6.5 Si-0.01 Pd as the basic composition, is an austenitic stainless steel, and has its corrosion resistance drastically improved due to the addition of silicon and palladium.

3. Corrosion resistance of new corrosion resistant stainless steel

3.1 Corrosion behavior of high-Si stainless steel and effect of the added elements

A screening test has been conducted to understand the effects of the concentration and temperature of sulphuric acid on the corrosion rate of various stainless steels, including the high-Si austenitic stainless steel and high-Cr austenitic stainless steel. The test results have shown that austenitic stainless steel with more than 5% Si content (hereafter "high-Si steel") has excellent corrosion resistance with the corrosion rate of lower than 0.1 mm/year in 373 to 473 K, 98% H_2SO_4, and can therefore be adopted as a material which meets the aforementioned requirements.

The corrosion rate in high-Si steel has been found to decrease with the increase in Si content within the range of 5 to 8%, improving the corrosion resistance. However, a wide range of additional elements such as transition metal, rare-earth element, semiconductor element, etc. have been tried to ascertain the effects of these elements, and to evaluate the corrosion resistance of high-Si steel, and the results have shown that palladium (Pd) is the element which improves the corrosion resistance most effectively.

In the case of high-Si steel, the higher the Pd content, the better the corrosion resistance within the range of 0.01 to 0.7%. **Fig. 1** shows the effect of Pd content on corrosion resistance in terms of the relationship with the Si content, indicating that the corrosion resistance zone with corrosion rate of lower than 0.1 $g/(m^2 \cdot h)$ gets narrowed as the temperature rises.

Furthermore, a high-Si content is needed in the high-temperature corrosion resistant zone, and with the Si content at high level, the effect of Pd addition gets more conspicuous, so that a slight addition of Pd can bring about the desired corrosion resistance. As will be mentioned later, from the standpoint of productivity, etc. the Si content seems to be limited to about 7%, suggesting that it is difficult to obtain the target of corrosion resistance simply by increasing the Si content.

Table 1 Chemical composition of new corrosion resistant stainless steel (Unit: mass%)

Material	C	Si	Mn	P	S	Ni	Cr	Pd
New corrosion resistant stainless steel	≤ 0.020	6.0/6.7	1.4/1.6	≤ 0.035	≤ 0.003	17.6/18.2	16.4/17.0	0.010/0.015

*1 Hiroshima Research & Development Center, Technical Headquarters
*2 Nagasaki Research & Development Center, Technical Headquarters
*3 Chemical Plant Engineering & Construction Center, Machinery Headquarters
*4 NKK CORPORATION

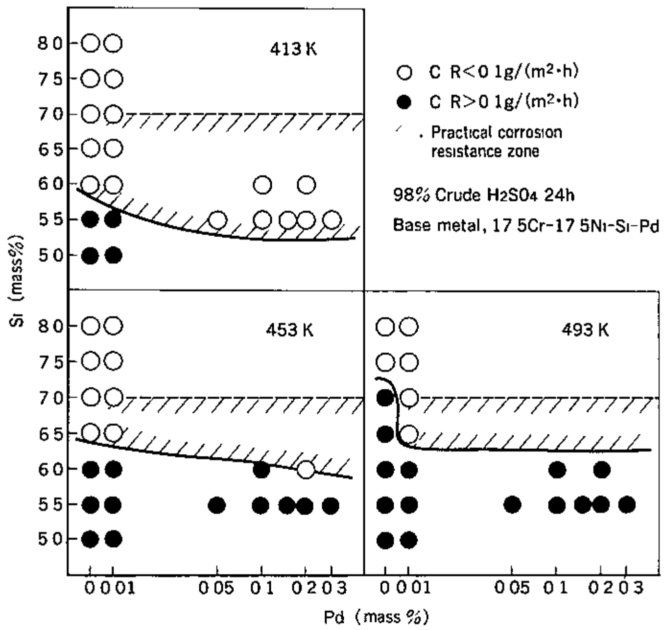

Fig. 1 Effect of Si and Pd contents on corrosion rate of stainless steel

The corrosion resistance is improved as the Si and Pd contents are increased, but the corrosion resistance zone with corrosion rate lower than 0 1g/(m² · h) gets narrowed as the temperature rises

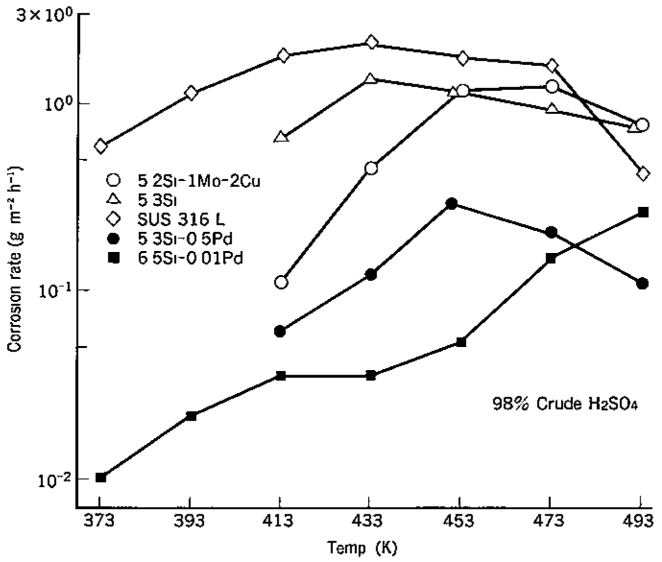

Fig. 2 Effect of temperature on corrosion rate of new corrosion resistant stainless steel

The new corrosion resistant stainless steel (6 5 Si-0 01 Pd) excels other steels in corrosion resistance, mostly satisfying the target level of corrosion rate lower than 0 1 mm/year

3.2 Corrosion resistance of high-Si stainless steel with Pd content

The results of corrosion tests of high-Si stainless steel with Pd content (hereafter "6 5 Si-0.01 Pd steel"), compared with other steels, are given in **Fig. 2**, indicating clearly that the 6.5 Si-0 01 Pd steel excels other steels in corrosion resistance and almost satisfies the target level with corrosion rate lower than 0 1 mm/year below 473 K, followed by the 5 3 Si-0 5 Pd steel

On the other hand, the 5 2 Si-1 Mo-2 Cu steel shows comparatively excellent corrosion resistance at 413 K, but is less resistant at higher temperatures over 413 K. The 5 3 Si steel and SUS 316 L are both inadequate in corrosion resistance at any levels of temperature of 413 to 493 K

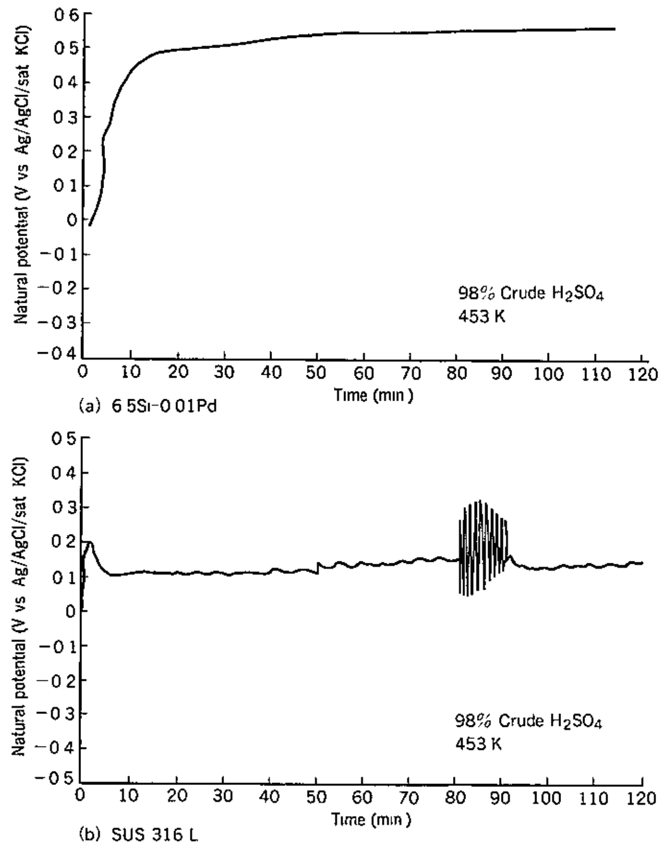

Fig. 3 Variation of corrosion potentials of stainless steels

The new corrosion resistant stainless steel shows slight potential fluctuation at the initial stage, with the potential being immediately stabilized

3.3 Corrosion resistance mechanism of new corrosion resistant stainless steel

Fig. 3 shows a representative example of variation of corrosion potentials of high-Si stainless steels with Pd content and other steels in high-temperature and high-concentration sulphuric acid It is clear from the Fig. that the 6.5 Si-0 01 Pd steel shows slight potential fluctuation just at the initial stage, with the potential getting immediately stabilized, and has therefore less potential fluctuation than the other steels Since the potential fluctuation implies transition of passive state and active dissolution[2], this indicates instability of the surface film. Hence, one of the reasons why the 6.5 Si-0 01 Pd steel has excellent corrosion resistance is the high stability of its surface film

The results of analyses such as ESCA after the corrosion test of high-Si steel with Pd have shown that the surface film is formed mainly of SiO_2, with Pd contained in the form of PdO It is assumed that the following corrosion reactions normally take place in high-temperature, high-concentration sulphuric acid[2].

(I) $m\mathrm{M} + n\mathrm{H_2SO_4} \rightarrow \mathrm{M}_m\mathrm{O}_n + n\mathrm{SO_2} + n\mathrm{H_2O}$,
formation of surface film

(II) $\mathrm{M}_m\mathrm{O}_n + n\mathrm{H_2SO_4} \rightarrow \mathrm{M}_m(\mathrm{SO_4})_n + n\mathrm{H_2O}$,
dissolution of surface film

where, M indicates Fe, Cr, Ni, Si, Pd, etc

The high corrosion resistance of the newly developed stainless steel is attributed to the oxides SiO_2 and PdO that form the surface film and are chemically stable in high-concentration sulphuric acid with a strong oxidation force Further, the result of the polarization measurement of 6 5 Si-0.01 Pd steel in high-temperature and high-concentration sulphuric acid of 453 K, 98% H_2SO_4 shows that the passivated current density is quite low as 5 $\mu A/cm^2$ when compared with 5 Si steel etc of 10 to 30 $\mu A/cm^2$

3.4 Evaluation of various corrosion resistance

The newly developed corrosion resistant stainless steel was subjected to a crevice corrosion test in high-temperature and high-concentration sulphuric acid of 473 K, 98% crude H_2SO_4, a corrosion test in flowing sulphuric acid, and a stress corrosion-cracking (SCC) test

A test piece with the multi-crevice type shape, complying with the ASTM standard, was used for the crevice corrosion test, a circular disc shape test piece with thickness 3 mm was used at flow velocity 1 to 6 m/s for the corrosion test in flowing sulphuric acid; and a U-bend test piece was used for the SCC test. The new corrosion resistant stainless steel did not show any symptom of corrosion during 8 424 hours of the crevice corrosion test And it showed notably less corrosion than Ni-alloy steels, etc (**Fig. 4**) during corrosion test in flowing sulphuric acid. Moreover, stress corrosion cracking did not initiate during 10 000 hours of the SCC test.

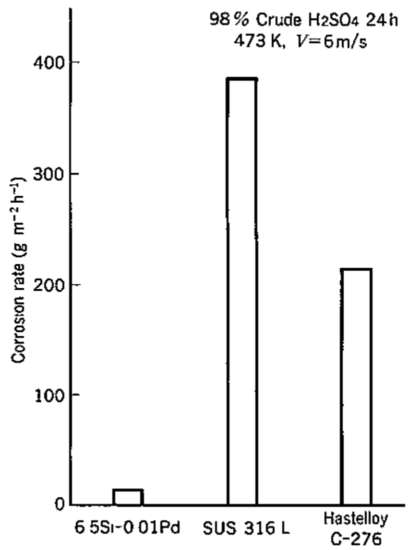

Fig. 4 Corrosion rate of stainless steels in flowing sulphuric acid
The new corrosion resistant stainless steel was found to have a notably lower corrosion rate in flowing sulphuric acid than the other steels

4. Workability of new corrosion resistant stainless steel

Because of the high-silicon content with 6.5% in the newly developed corrosion resistant stainless steel, the segregation of Si was apprehended at the time of rolling. Hence, the workability of hot rolling was examined through a soaking test and a thermomechanical simulated tensile test (hereafter "thermomechanical F tensile test"). The 25 kg and 50 kg ingots were vacuum melted for the test

The specimens were subjected to δ-ferrite content variation by adjusting the Ni content, with the Si content set at 6.7% Comparison was made with the steels having lower Si contents with 6 2% and 5% The test piece for thermomechanical F tensile test was cut off from the as cast ingot, and heating temperature was 973 to 1 523 K

In the soaking test, the dice-shaped test piece was cut off from the ingot, was kept heated to 1 373 to 1 523 K for 1 to 200 h before air-cooling to measure the composition, hardness and δ-ferrite content From the result of the thermomechanical F tensile test of the as cast material, the nil ductility temperature of 6% Si steel is nearly 1 373 K, with the reduction of area at 1 173 to 1 273 K being reduced to 50%, indicating that 6% Si steel is not good in terms of hot workability (**Fig. 5**) From the soaking test result, the second phase metallic microstructure was found to have almost disappeared, with the uniform austenitic microstructure appearing when heated up to 1 373 K for over 10 h, but requiring longer time when the temperature is higher than 1 373 K Compared to the as cast material, the specimen used for the soaking test at 1 373 K for 100 to 200 h does show an increase in reduction of area and an improvement of hot workability, but little change is seen in the nil ductility temperature (Fig 5) On the basis of the aforementioned test results, and from the result of rolling tests on the soaking material, we have deduced that stainless steel containing 6 to 7% Si can be put to rolling

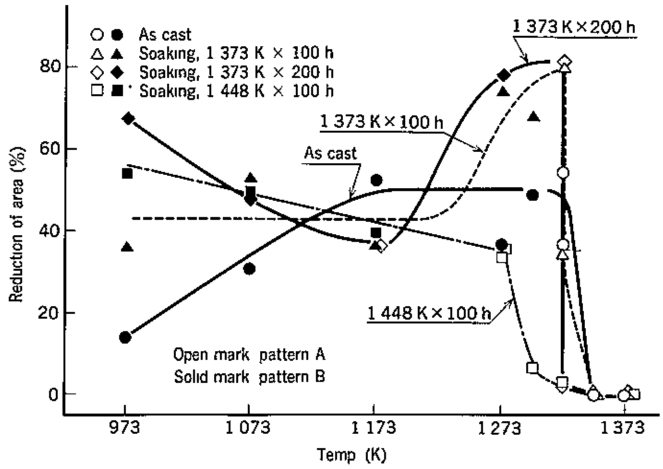

Fig. 5 Hot workability of new corrosion resistant stainless steel
Compared with the as cast material, the material subjected to a soaking treatment shows an increase in reduction of area and improvement in hot workability

5. Weldability

5.1 Weldability and crack resistance

The tensile test, the impact test and the T-type fillet weld cracking test, carried out on the new corrosion resistant stainless steel welded joint due to TIG welding, have shown that the newly developed stainless steel has the weldability equivalent to, or higher than, conventional stainless steels such as SUS 309, SUS 316 L, etc Furthermore, the newly developed stainless steel shows slight crater cracks in the T-type fillet weld

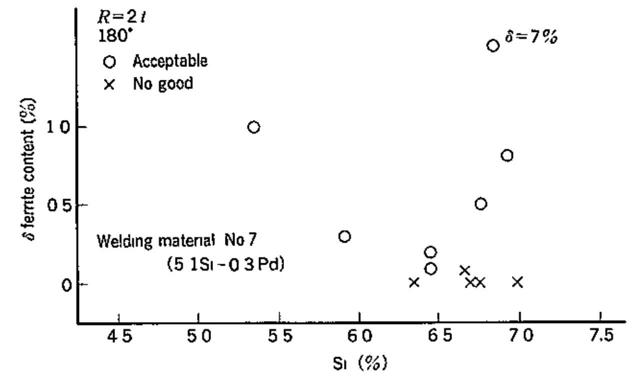

Fig. 6 Effect of Si and δ ferrite contents of base metal on bending ductility at welded joint

Bending ductility is clearly improved when the δ-ferrite content in the base metal is over 0 3%

Table 2 Effect of Si content of base metal and welding material on bending ductility of welded joint

Base metal (δ ≧ 0 1%)

		(δ = 0 1)			(δ = 0 7)		(δ = 0 8)
	Si (%)	6 4	6 5	6 6	6 7	6 8	6 9
Welding material							
No 7	5 1	◎			◎		○
W 1	5 5	◎					
W 2	6 0	○					
W 3	6 1	×					

16 to 17 Cr type
No 7 16 92 Cr-16 55 Ni-5 10 Si-0 27 Pd, Ni-bal = −4 32
W 1 16 80 Cr-16 35 Ni-5 51 Si-0 52 Pd, Ni-bal = −4 95
W 2 16 98 Cr-17 65 Ni-6 07 Si-0 20 Pd, Ni-bal = −5 18
W 3 16 78 Cr-17 88 Ni-6 13 Si-0 43 Pd, Ni-bal = −4 69
Bending ductility R = 2 t, 180
◎ Excellent, t = 15 mm, ○ Excellent, t = 5 mm, × Inadequate, t = 5 mm

test and micro-cracks in multi-layered weld cracking test, but hardly any cracks were seen in butt welded joint, indicating that the steel has considerably higher crack resistance

5.2 Ductility of welded joint

Because of the conspicuously high-Si content in the new corrosion resistant stainless steel, welding material with lower Si and higher Pd contents than the base metal was adopted

The results of EPMA analysis, EDS analysis, etc on the welded joint showed enriched phases of Ni and Si at the same place of the bond in the welded joint with poor bending ductility, suggesting the formation of a Ni-Si type intermetallic compound Therefore, the HAZ of the base metal forming the bond was reproduced to evaluate the mechanical properties The 5 3% Si steel with excellent bending ductility, the 6 9% Si steel containing δ-ferrite, and the 6 7% Si steel poor in ductility and with δ lower than 0 1% were used as the specimens for the test With the thermal history, same as the one at the time of producing the welded joint, applied to the aforementioned specimens to evaluate the ductility (reduction of area), the ductility was found to deteriorate as the precipitation of the supposed Ni-Si type intermetallic compound phase increased

Fig. 6 shows the result of the bending test of the welded joint produced by using the same welding material with the base metals differing in Si and δ-ferrite contents. As is clear from the figure , the bending ductility is improved when the δ-ferrite content in the base metal is over 0 3%. However, in the case where the base metal has the Si content less than 6.5%, the ductility is sufficiently high even when the δ-ferrite content is approximately 0 1%

It can be deduced that the welded joint has excellent ductility when the Si content in the welding material is less than 6% against the base metal with δ-ferrite content exceeding 0 1% (**Table 2**). Furthermore, it has been revealed, through the relationship of δ-ferrite content and Ni-balance of the weld metal, that excellent bending ductility can be obtained when the δ-ferrite content is higher than the 5% level Moreover, no distinct correlationship has been found between the bending ductility of the welded joint and the hardness of the weld metal

From the aforementioned results, it can be deduced that the new corrosion resistant stainless steel ensures excellent weldability and ductility, by controlling the Si content, δ-ferrite content, etc. in base metal and welding material, while requiring no preheating or post weld heating treatment.

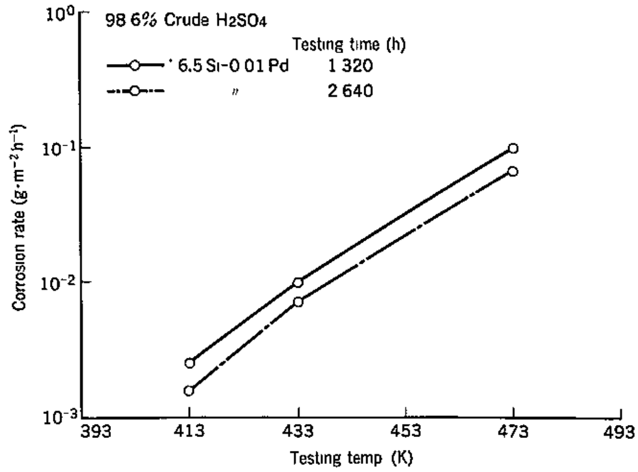

Fig. 7 Corrosion rate of new corrosion resistant stainless steels in loop test

The new corrosion resistant stainless steel shows excellent corrosion resistance in flowing crude sulphuric acid inside a loop testing apparatus

6. Actual corrosion test

In order to evaluate the corrosion resistance of the new corrosion resistant stainless steel in an actual crude sulphuric acid solution environment, the testing apparatus made of the newly developed stainless steel was installed in an actual sulphuric acid production plant to carry out the loop test. Furthermore, the corrosion test was also conducted by partially employing the new corrosion resistant stainless steel for the pipe between the absorption tower and the cooler in an actual plant In the case of the loop test, 98.5% crude sulphuric acid at 353 K was fed into the loop testing apparatus through the existing cooler pipe, and was circulated inside the apparatus before being returned back to the cooler. The three containers inside the testing apparatus were heated respectively to 413 K, 433 K and 473 K, and a fast flowing section was installed And, the reduction in pipe thickness was measured when 98 to 99% crude sulphuric acid at 363 K flowed through the pipe All tests were carried out for about one year **Fig. 7** shows the result of immersion test carried out inside the loop testing apparatus, clearly indicating that the higher the testing temperature, the higher the corrosion rate of the new corrosion resistant stainless steel, with the trend being the same as in the laboratory test However, the newly developed steel has proved to satisfy the target values and ensure excellent corrosion resistance The pipe made of this steel shows little reduction in thickness, and is excellent in corrosion resistance

7. Conclusion

The newly developed corrosion resistant stainless steel for sulphuric acid plants has the features given below

(1) The new corrosion resistant stainless steel with 6% silicon content ensures an outstanding corrosion resistance with corrosion rate less than 0 1 mm/year in high-temperatures and high-concentration sulphuric acid of 373 to 473 K, 98%, by adding a small amount of palladium Moreover, the steel shows excellent corrosion resistance in flowing sulphuric acid, and ensures excellent crevice corrosion resistance and SCC resistance.

(2) In spite of the high-Si content, the newly developed stainless steel can be used as the rolled steel simply by carrying out a soaking treatment

(3) The new corrosion resistant stainless steel ensures substantial weldability and welded joint ductility by adding over 0.3% δ-ferrite in the base metal, and by adjusting the welding material to make the Si content lower than the base metal, by adding a higher content of palladium, and by making the δ-ferrite content higher than 5%.

(4) The new corrosion resistant stainless steel shows a low corrosion rate of less than 0 04 mm/year in the loop test, etc. carried out in an actual crude sulphuric acid plant environment, and ensures higher corrosion resistance than conventional steels

References

(1) New materials—the acid test, Sulphur No.201, (1989) p 23

(2) Nemoto, R et al , Corrosion Behavior of Stainless Steel in Concentrated Sulphuric Acid, Boshoku Gijutsu (Corrosion Engineering), Vol 34 (1985) p 708

MITSUBISHI TECHNICAL BULLETIN, ALREADY ISSUED

E: in English

111 E Study on Treatment of Tanker Discharged Oily Water with Improved Type Slop Tank, 1976
112 E Prediction of NOx Emission from Boiler Furnaces and Development of Extremely Low NOx Burner, 1976
113 E Study on Extremely Low NOx Burners for Chemical Furnaces, 1976
114 E Digital Dynamic Simulation Program Especially Designed for Heat Exchanger Processes "HEDDY", 1976
115 E A Power Prediction Method for High Block Coefficient Ships with Transom Stern, 1976.
116 E On the Unusual Phenomena in Manoeuvring Motions of a Full Ship Model, 1976
117 E Unsteady Cavitation of Oscillating Hyfrofoil, 1977
118 E "Mitsubishi Galant Σ," a New Passenger Car, 1977
119 E Some Investigations on Propeller Open-Water Characteristics for Analysis of Self-Propulsion Factors, 1977
120 E Axial Flow Compressors for Base-Load LNG Liquefaction Plants, 1977,
121 E An Outline of Our Research Organization on Ocean Engineering Techniques, 1977
122 E Changes in the Properties of Solid Solution Hardened and Dispersion Strengthened Ni-Base Superalloys by Long Term Heating, 1977
123 E Development of Wet Type NOx Removal Processes, 1977
124 E Development of NOx Removal Process with Catalyst for Stationary Combustion Facilities, 1977
125 E Numerical Evaluation of a Wave-Resistance Theory for Slow Ships, 1978
126 E Continuous System Simulation Program "MDAS/4" Especially Designed for Stiff Problems, 1978
127 E Vibration Analysis of Axi-symmetric Shell by Mode Superposition, 1978
128 E Low Pressure Turbine Test Facility, 1978
129 E Corrosion Fatigue Behavior of 13 Cr Stainless Steel for Turbine Moving Blade, 1978
130 E Vanishing Temperature of Back Corona with High Resistivity Fly Ash in Hot-Side Electrostatic Precipitation, 1979
131 E Design of Supercritical Pressure Steam Generator for Middle Load Use, 1979
132 E Development of Low Circulation Ratio Controlled Circulation[R] Boiler 1979
133 E Comparison between Calculated and Measured Results of Turbulent Boundary Layers around Ship Models, 1979
134 E Development of Super-Low NOx PM Burner, 1979
135 E Study on the Behavior of Corrosion of Inconel 600 Alloy in High-temperature Sodium Phosphate Solution, 1979
136 E Corrosion-resistance of Inconel 600 under AVT Conditions, 1979
137 E Prediction and Model Experiments on Speed Loss of a Ship in Waves 1979
138 E Training Simulator for Compressor Plants, 1980
139 E Control of Gas Side Corrosion in Oil Fired Boilers 1980
140 E Effect of Air Bubbles Entrained from Bow on Propeller-induced Pressure Fluctuation, 1980
141 E Computer Aided Stress Analysis System for Nuclear Plant Primary Components, 1980
142 E Multiple Fuel Firing Controlled-Circulation Boiler Using Rifled Tubing, 1980
143 E Practical Approach to Unsteady Problems of Marine Propellers by Quasi Steady Method of Calculation, 1980
144 E Innovated Operation Systems of Container Terminal, 1981
145 E Standard Method of Measurement and Analysis of Speed Trial Data in Nagasaki Experimental Tank, 1981
146 E Tribological Study on Machine Elements of HTGR Components 1981
147 E Fracture Mechanics Analysis of Independent Prismatic Tank of Low Temperature LPG Carrier for Verification of IMCO Type B, 1981
148 E An Application of Building Block Method to Vibration Problem of Diesel Powered Ship 1982
149 E Studies on Analytical Method and Nondestructive Measuring Method on the Sensitization of Austenitic Stainless Steels, 1982
150 E A Method to Predict Fluctuating Pressures Induced by a Cavitating Propeller 1982
151 E Response Analysis of Tension Leg Platform with Mechanical Damping System in Waves, 1982
152 E Ultrasonic Testing of Austenitic Stainless Steel Welds, 1982
153 E Improvement of ISI Techniques by Multi Frequency Eddy Current Testing Method for Steam Generator Tube in PWR Plant, 1982
154 E Hydrodynamic Design and Development of High Speed Craft in MHI, 1982
155 E Structural Design of Large Aluminum Alloy High Speed Craft, 1983
156 E Production of "YOZO" Tubes of Special Shapes, 1983,
157 E A Study on Creep Fatigue Life Prediction Using Simple High Temperature Low Cycle Fatigue Testing Machines 1983
158 E Study on Motions of Floating of Bodies under Composite External Loads, 1983
159 E Improvement of Material Properties of Ni Base Alloy Investment Castings by Hot Isostatic Processing, 1983

160 E Total System for Prediction of Seakeeping Qualities of Ships (Prediction of Ship Motions, Wave Load etc. and Its Application to Design), 1983

161 E A Study on Evaluation of Print Quality, 1983

162 E Technical and Economic Aspects of Arctic Marine Transportation—A State of the Art—, 1984

163 E Development of a Ni-base Heat Resistant Alloy (TOMILLOY) for Gas Turbine Combustor, 1984

164 E Historical Review of Research and Development in Ship Hydrodynamics, 1984

165 E Development for the Measurement of Ink Film Thickness and Dampening Water Content, 1984

166 E Application of Ship Resistance Theories to the Design of Full Hull Forms, 1985

167 E Behavior of Impurity around the Ion Exchanger in PWR Primary Circuit, 1985

168 E Effect of Bow Shape on Free Surface Shear Flow, 1985

169 E Study on Detection of Deterioration and Damage due to High Temperature Service Using Nondestructive Material Property Tests, 1985

170 E Ice Milling Loads Encountered by a Controllable Pitch Propeller, 1985

171 E Fracture Surface Analysis of Cast Irons, 1985

172 E Studies on Fluid Structural Vibration Using Boundary Element Method, 1986

173 E Evaluation Method of the Brittle Fracture Strength in Structurally Stress-Concentrated Regions, 1986

174 E Study of Ice Forces for Offshore Structures, 1987

175 E Some New Fatigue Tests in High Temperature Water and Liquid Sodium Environment, 1987

176 E A Study on the Mechanical Behavior of Soil During Flat Edge Cutting, 1987

177 E Second Bosporus Bridge, 1987

178 E Study on Fiber Cleaning Technology by Means of Solvent Replacement, 1987

179 E Vibration Analysis of Superstructure by Mode Synthesis Method, 1988

180 E A Simulation Study on Ship Manoeuvrability at Low Speeds, 1988

181 E Dynamic Blade Stress on Marine Propellers Operating in Wake of Ship's Hull, 1988

182 E Application of Super 9 Cr Steel Large Diameter and Thick Wall Pipes, 1988

183 E Development of the Mitsubishi UEC75LSII Type Diesel Engine, 1988

184 E Development of Polymeric Shape Memory Material, 1988

185 E Study on the Seismic Response of Reactor Vessel of Pool Type LMFBR Including Fluid-Structure Interaction, 1988

186 E Study of Flow-Induced Vibrations of a Sieve Tray Column, 1988

187 E Design and Operating Results of 145 MW Low Caloric Gas Fired Combined Cycle Power Plant for Chiba Works of Kawasaki Steel Corporation, 1989

188 E Simulation of Sound Field Using Boundary Element Method, 1989

189 E Study on Vibratory Response of Deck in Superstructure, 1989

190 E A Study of Excavatability Index for B.W.E., 1989

191 E Turbine Performance Improvement by Full 3-D Design Blades, 1989

192 E Design of LNG Fired USC Steam Generator for Units Nos.1 & 2 of Kawagoe Power Station, Chubu Electric Power Co., Inc., 1989

193 E BEM-FEM Hybrid Stress Analysis, 1990

194 E Development of Overlapping Modelling for Atmospheric Diffusion, 1991

195 E A Surface Panel Method with a Deformed Wake Model to Analyze Hydrodynamic Characteristics of Propellers in Steady Flow, 1991

196 E Influence of Gear Mating Contact Ratio on Vibration and Noise of Cylindrical Gear System, 1991

197 E Gates and Penstocks for Samanalawewa Project, 1991

198 E Stochastic Seismic Response Analysis of Structures with Uncertain Properties, 1992

199 E Development of Oil-Free Centrifugal Compressor, 1992

200 E Microwave Excited CO_2 Laser, 1993

201 E Development of New Corrosion Resistant Stainless Steel for Sulphuric Acid Plant, 1996

Published by
Technical Administration Section, Technical Administration Dept., Technical Headquarters,
MITSUBISHI HEAVY INDUSTRIES, LTD., 3-1, Minatomirai 3-chome, Nishi-ku, Yokohama, Japan

Printed in Japan © 1996